Free Rad. Res., Vol. 28, pp. 517–532
Reprints available directly from the publisher
Photocopying permitted by license only

ESR Studies of a Series of Phthalocyanines. Mechanism of Phototoxicity. Comparative Quantitation of $O_2^{\bullet -}$ using ESR Spin-Trapping and Cytochrome c Reduction Techniques

ANGELE VIOLA [a], ANDRE JEUNET [b], RICHARD DECREAU [a], MICHEL CHANON [a] and MICHEL JULLIARD [a,*]

[a] *Laboratoire AM³-ESA 6009, Faculté des Sciences Saint-Jérôme, 13397 Marseille cedex 20, France;* [b] *LEDSS, UMR 5616, 301 avenue de la Chimie, Domaine Universitaire de Grenoble, 38041 Saint-Martin d'Hères, France*

Accepted by Prof. S. Steenken

(Received 18 April 1997; In revised form 27 October 1997)

ESR experiments with 2,2,6,6-tetramethyl-4-piperidone (4-oxo-TEMP) and the spin-trap 5,5-dimethyl pyrroline-N-oxide (DMPO) have been performed on a series of new phthalocyanines: the bis(tri-*n*-hexylsiloxy) silicon phthalocyanine ($[(nhex)_3SiO]_2SiPc$), the hexadecachloro zinc phthalocyanine ($ZnPcCl_{16}$), the hexadecachloro aluminum phthalocyanine ($AlPcCl_{16}$), the hexadecachloro aluminum phthalocyanine sulfate ($HSO_4AlPcCl_{16}$), whose photocytotoxicity has been studied against various leukemic and melanotic cell lines. Type I and Type II pathways occur simultaneously in DMF although the Type II seems to be prevalent. These results are not changed when the bis(tri-*n*-hexylsiloxy) silicon phthalocyanine is entrapped into liposomes. By contrast, the Type I process is favored in membrane models for all the perchlorinated phthalocyanines. This modified behavior may be accounted on a possible stacking of phthalocyanines in membranes and a preventing effect of axial ligands against aggregation in the case of the bis(tri-*n*-hexylsiloxy) silicon phthalocyanine. The photodynamic action of zinc perchlorinated phthalocyanine is not dependent on singlet oxygen, phototoxicity of this molecule being essentially mediated by oxygen free radicals. Quantitation of the superoxide radical was accomplished, with good agreement, by two techniques: the cytochrome c reduction and the ESR quantitation based on the double integration of the first derivative of the ESR signal. The disproportionation of the superoxide radical or degradation of the spin-trap seem to be avoided in aprotic solvents such as DMF.

Keywords: Phthalocyanine, photosensitization, photodynamic therapy, active oxygen, superoxide radical quantitation, ESR, spin-trapping, cytochrome c

Abbreviations: AlClPc, aluminum chlorophthalocyanine; $AlPcCl_{16}$, hexadecachloro aluminum phthalocyanine; Carbamoyl PROXYL, 3-carbamoyl-2,2,5,5-tetramethyl-1-pyrrolidine-1-yloxy free radical; DMPO, 5,5-dimethyl-1-pyrroline-N-oxide; DETAPAC, diethylenetriaminepentaacetic acid; DPPC, DL-α-dipalmitoylphosphatidylcholine; ESR, Electron Spin Resonance; $HO_2^{\bullet}$, perhydroxyl radical; $HSO_4AlPcCl_{16}$, hexadecachloro aluminum phthalocyanine sulfate; $[(nhex)_3SiO]_2SiPc$, bis(tri-*n*-hexylsiloxy) silicon phthalocyanine; $^1O_2$: singlet oxygen; $O_2^{\bullet -}$, superoxide radical; $^{\bullet}OH$, hydroxyl radical; 4-oxo-TEMP, 2,2,6,6-tetramethyl-4-piperidone; 4-oxo-TEMPO, 2,2,6,6-tetramethyl-4-piperidone-N-oxyl;

* Corresponding author. E-mail: michel.julliard@am3.u-3mrs.fr.

PDT, photodynamic therapy; SOD, superoxide dismutase; $ZnPcCl_{16}$, hexadecachloro zinc phthalocyanine

INTRODUCTION

Photodynamic therapy (PDT) is an experimental treatment modality suitable for various malignant tumors.[1–5] The tumoricidal potency of this procedure is based on the capacity of certain photosensitizers (light absorbing compounds) to preferentially stain neoplastic tissues versus normal tissues. Subsequent irradiation of the tumor with visible light of specific wavelength consistent with the absorption maximum of the dye, induces light activation of the photosensitizer. The excited chromophore reacts with biomolecules or oxygen in its vicinity generating potent toxicants (such as oxygen-derived cytotoxic species) eliciting thereby abnormal tissues while sparing healthy adjacent areas slightly strained and/or non-irradiated.[6–9] The excited state of the photosensitizer may undergo a photoinduced electron transfer (reductive or oxidative) and/or exchange an hydrogen atom, producing radicals and active oxygen species such as the superoxide ($O_2^{\bullet -}$) and the hydroxyl ($^{\bullet}OH$) radicals. This pathway is termed as a Type I process. The excited state can also transfer energy to dioxygen, in a so-called Type II[10–12] mechanism generating $^1O_2$ (Figure 1). There are few examples of excited photosensitizers acting simultaneously both through Type I and Type II mechanisms.[13–18] Although, there is much experimental evidence that $^1O_2$ is a major reactive intermediate generated in the primary photochemical process, direct monitoring of this species in biological systems is still difficult to achieve.[19–21] The generation of oxygen free radicals has however been demonstrated in cells photosensitized by phthalocyanines.[22] Superoxide $O_2^{\bullet -}$ and $^{\bullet}OH$ radicals are involved in a variety of deleterious effects on cells owing to the high reactivity of $^{\bullet}OH$.[23] The superoxide radical anion is not only involved in the generation of $^{\bullet}OH$ but is also directly responsible for some destructive processes.[23] Moreover, the combined action of oxygen free radicals and biological reducers was recently postulated to be of importance in cell photosensitization.[24–26]

The first generation sensitizers such as metalloporphyrins and Photofrin II which is the only photosensitizer approved for clinical use suffer from major drawbacks: a lack of chemical purity, too weak red light absorption, a long period of enhanced cutaneous sensitivity to sunlight following systemic administration. Hence there is considerable effort to find new chemically pure photosensitizers activated by longer wavelengths and able to lead to higher penetration.

We present in this paper a comparative study of new perchlorinated phthalocyanines: the hexadecachloro zinc phthalocyanine ($ZnPcCl_{16}$), the hexadecachloro aluminum phthalocyanine ($AlPcCl_{16}$), the hexadecachloro aluminum phthalocyanine sulfate ($HSO_4AlPcCl_{16}$) and a silicon phthalocyanine derivative: the bis(tri-*n*-hexylsiloxy) silicon phthalocyanine ($[(nhex)_3SiO]_2$ SiPc). Noteworthy features of phthalocyanines are their elevated absorption in the red spectral region, their high $^1O_2$ quantum yield and their powerful photosensitizing properties. The main rationale behind the synthesis of these new phthalocyanines was that appropriate modification such as chlorination would theoretically enhance the $^1O_2$ quantum yield via the heavy-metal effect. The bis-(tri-*n*-hexylsiloxy) silicon phthalocyanine was designed with axial hexyl chains to prevent aggregation of the dye and to enhance its lipophilicity. With regard to the potential antineoplastic properties of these molecules[27,28] it was essential, from the viewpoint of elucidating primary phototoxic effects, to determine the exact nature of the oxygen species produced by these photosensitizers. This was accomplished both in air saturated solutions and in synthetic membrane models such as liposomes made from DL-α-dipalmitoylphosphatidylcholine (DPPC). We used electron spin resonance spectroscopy (ESR) with 2,2,6,6-tetramethyl-4-piperidone

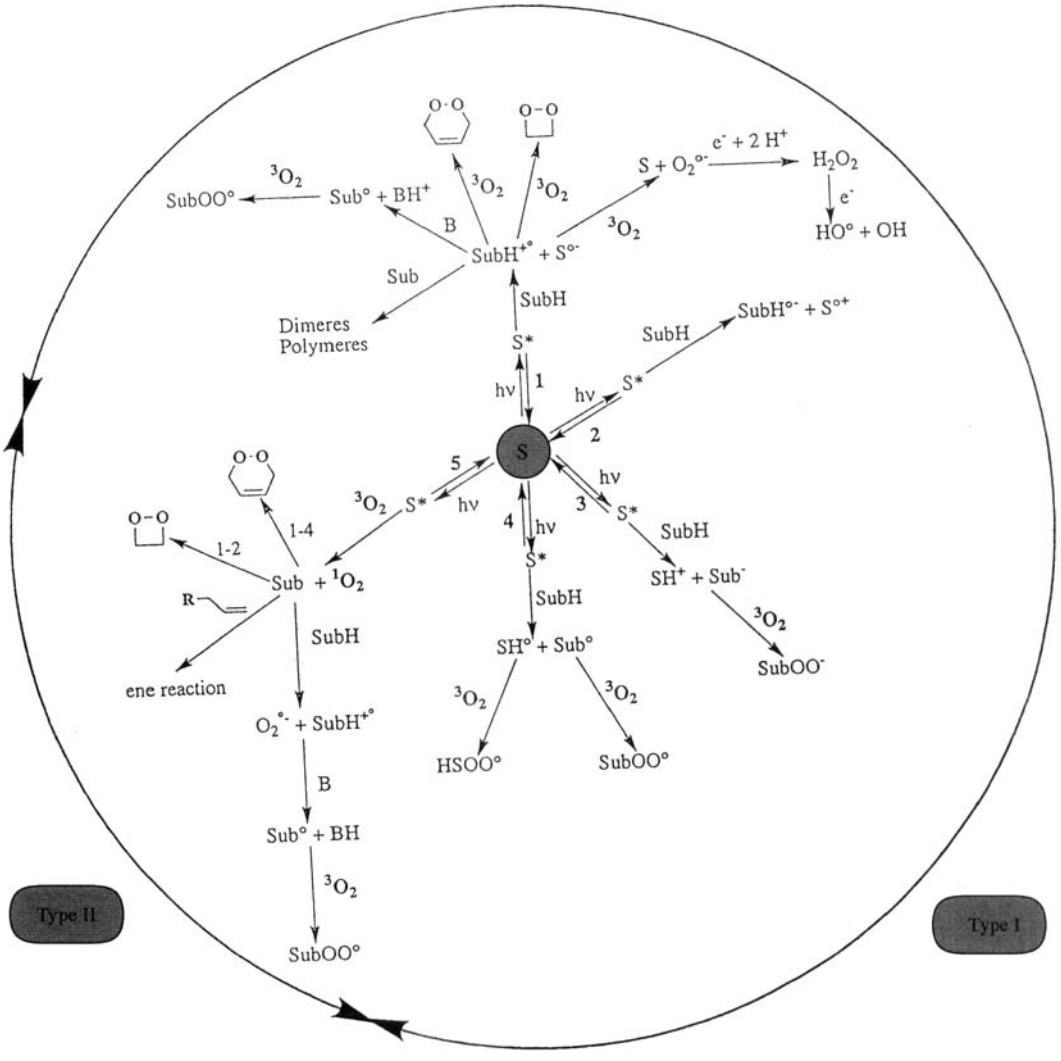

FIGURE 1 Possibilities for a photosensitizer (S) to generate radicals in an aerobic biological medium. In arrows 1 and 2 the light increases the oxidation and/or oxidizing abilities of the photosensitizer. In arrow 3 it increases the acid and/or base properties of the photosensitizer (only the second shown). S*, more basic, can abstract a proton from a substrate Sub leading to Sub^- which can couple to $^3O_2$ affording $SubOO^-$. In arrow 4 the light transforms S into a reagent displaying increased tendency to effect SH_2 reactions. In arrow 5, S becomes a reservoir of energy able to transform $^3O_2$ into $^1O_2$. S: sensitizer; S*: photoexcited sensitizer; Sub: unsaturated substrate; SubH: substrate containing an atom of hydrogen; B: base.

(4-oxo-TEMP) to check the generation of $^1O_2$, and the spin-trapping technique to detect and study short-lived intermediates such as $O_2^{\bullet -}$ and $^\bullet OH$. Quantitation of the superoxide radical has also been performed with two different techniques: the cytochrome c assay and ESR spectroscopy.

MATERIALS AND METHODS

Chemicals

The aluminum chlorophthalocyanine was purchased from Eastman Kodak and used as supplied. $[(nhex)_3SiO]_2SiPc$ was synthesized as

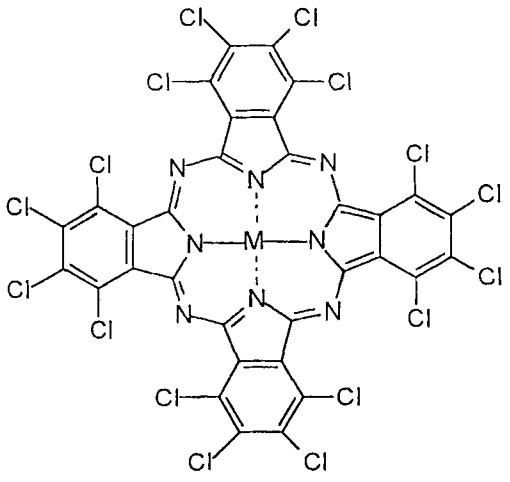

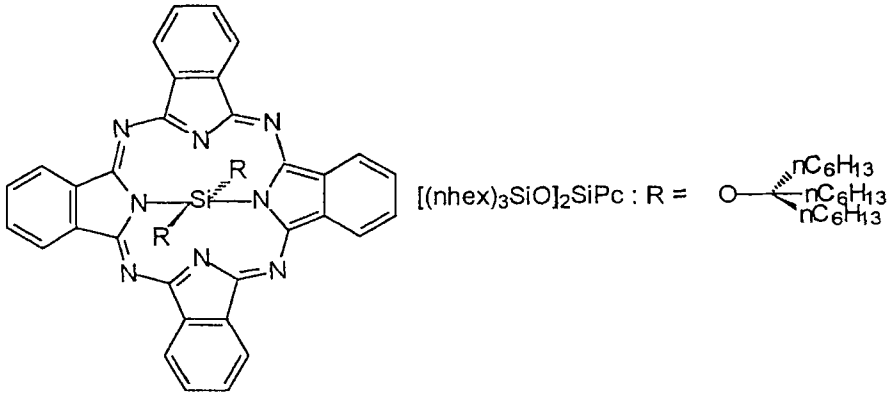

FIGURE 2 Chemical structure of the different photosensitizers.

described previously.[29,30] The perchlorinated phthalocyanines derivatives ($ZnPcCl_{16}$, $AlPcCl_{16}$, $HSO_4AlPcCl_{16}$) were prepared according to the method of Golovin *et al.*[31] Chemical structures of the phthalocyanines are shown in Figure 2. The 5,5-dimethyl-1-pyrroline-N-oxide (DMPO), 4-oxo-TEMP, 3-carbamoyl-2,2,5,5-tetramethyl-pyrrolidine-1-yloxy free radical (Carbamoyl PROXYL) were from Aldrich. All these products were used without further purification with the exception of DMPO which was distilled[32] before use and stored under an argon atmosphere at −20°C. The purified DMPO was routinely checked to ensure that no ESR contaminating signal adduct was present. We also verified before each quantitative measurement that no undesirable set of lines consisting of a triplet of doublets assigned to a DMPO derivative impurity[33] would superimpose on the spectra. Histidine, D_2O were purchased from Aldrich company. Ferricytochrome c, superoxide dismutase (SOD), catalase, DPPC (C16:0; DPPC) were obtained from Sigma. Desferrioxamine B as a lyophilized powder was from Ciba-Geigy. Stock solutions were made up fresh in phosphate buffer. Stock solutions of Fe–DETAPAC (iron (III)) were

prepared[34] with diethylenetriaminepentaacetic acid and $FeCl_3$ from Aldrich. Phosphate buffer saline (PBS) (pH 7.4) was obtained from Biowittaker. Chelex 100 chelating ion exchange resin (50–100 mesh) from Bio-Rad. The solvents used for spectroscopy and ESR experiments, namely *N,N*-dimethylformamide (DMF), dimethylsulphoxide (DMSO), acetonitrile were all spectrophotometric grade (Aldrich).

Preparation of Solvents and Buffers for Quantitative Measurements

DMSO was treated with CaH_2 overnight and then dried on molecular sieves (4 Å). Dimethylformamide was also dried on molecular sieves. To remove any trace of adventitious divalent cation before use, PBS was gently stirred for 1 h with Chelex resin and then filtered after decantation.

Liposomes Preparation

DPPC was used to prepare liposomes according to the injection technique.[35] DPPC (3.67×10^{-4} M) was injected in 10 ml of a PBS solution. The average diameter of liposomes obtained using this technique was 25 nm as measured with electron microscopy.[35] DMF solutions of DMPO or TEMP were injected simultaneously with DMF phthalocyanine solutions into the DPPC preparation.[36] The final concentration of dye in the liposomal suspension was 2×10^{-5} M.

Irradiation Procedures

Irradiation was carried out using a 250 W halogen lamp, which exhibits an emission maximum centered between 600 and 700 nm (ORIEL, USA). Light intensity in the central area of the illuminator was about 10 mW/cm^2 as determined by chemical actinometry as elsewhere described.[37] This light matches the maximum absorption peak of these phthalocyanines in the visible region of the spectrum (Table I). Absorption spectra of the various phthalocyanines were recorded on a Kontron Uvikon 930 spectrophotometer.

TABLE I Wavelengths of absorption maxima and values of molar extinction coefficients for the studied phthalocyanines

Photosensitizer	λ max (nm)	ε ($M^{-1}cm^{-1}$)
$[(nhex)_3SiO]_2SiPc$	668	3.1×10^5 (DMF)
$ZnPcCl_{16}$	666,692	2.5×10^4 (DMF)
$AlPcCl_{16}$	700	2.4×10^4 (DMF)
$HSO_4AlPcCl_{16}$	705	2.4×10^5 (DMF)

ESR Experiments

ESR spectra were recorded with a BRUKER ESP 300 E spectrometer at room temperature (22–24°C), microwave: 20 mW; modulation amplitude: 1.243 G; time constant: 40.96 ms, scan rate: 167.772 s; scan width: 100 G, X band, modulation frequency: 100 kHz. Photoinduced ESR spectra were obtained from the samples (150 µl) introduced into quartz capillaries specially designed for ESR analysis and directly irradiated inside the microwave cavity. Anaerobic experiments were carried out in closed vials after purging the solutions with argon for 15 min.

ESR Determination of Singlet Oxygen Generation

The ESR detection of singlet oxygen was performed by the oxidation of 4-oxo-TEMP (Scheme 1). The oxidation of this amine occurs at a rate constant varying in the range of 4×10^7–8×10^7 $M^{-1}s^{-1}$ and yields specifically the nitroxide radical: 2,2,6,6-tetramethyl-4-piperidone-N-oxyl radical (4-oxo-TEMPO).[38,39] However, we could not quantify the $^1O_2$ production via 4-oxo-TEMPO formation. Actually, a previous study in aqueous solution reported that 4-oxo-TEMPO is not convenient for precise quantitative measurements.[40] There is no quantitative ratio between the amount of $^1O_2$ and the yield of radical resulting from the oxidation of 4-oxo-TEMP. This was attributed to the slow homolytical breakage of the O–O bond of the 4-oxo-TEMPO hydroperoxide initially formed[40] (Scheme 1).

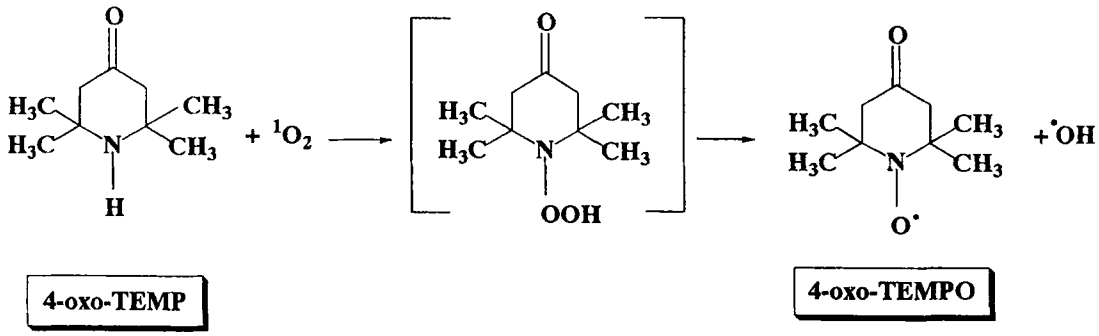

SCHEME 1

Quantitative Determination of the DMPO–OOH Adduct Yield

Knowledge of DMPO efficiency to trap $O_2^{\bullet -}$ in dried DMSO (91%) enabled ESR quantitative studies of $O_2^{\bullet -}$ generated by various phthalocyanines in this solvent.[14] However, it was not possible to take direct advantage of these results in so far as our dyes were not soluble ($AlPcCl_{16}$, $HSO_4AlPcCl_{16}$) or stable ($[(nhex)_3SiO]_2SiPc$) enough in DMSO. DMF was found to be convenient for all the phthalocyanines and was used as the common solvent for each ESR quantitative experiment.[41] We have determined the efficiency of DMPO to trap superoxide in this solvent following a published procedure[14] using KO_2 (0.2×10^{-3} M) as a source of $O_2^{\bullet -}$. We used this method with a modification for the cytochrome c assay. Actually cytochrome c is not stable in DMF and this drawback did not permit an immediate correlation between ESR and colorimetric results. This difficulty was overcome by comparing the double integration of the first derivative of the ESR signals recorded after adding an aliquot of the KO_2 solution to DMPO (0.15×10^{-3} M) in DMSO and in DMF. The 3-carbamoyl-2,2,5,5-tetramethyl-1-pyrrolidine-1-yloxy free radical was used as the radical standard to determine radical concentrations. The cytochrome c assay was feasible in DMSO and was related to the ESR calculations. Taking into account the percentage of error occurring in the double integration calculations[42] (±10%) the final results evidenced the same yield of trapping in DMSO as in DMF. DMPO is also efficient in trapping the hydroxyl radical, giving rise to the DMPO–$^{\bullet}$OH adduct. However, there may be some pitfalls in the trapping of the hydroxyl radical with DMPO. An artifactual hydroxyl production may occur from the spontaneous breakdown of DMPO–$^{\bullet}$OOH into DMPO–$^{\bullet}$OH (Scheme 2). This process is however often negligible.[43,44] Recently, new findings demonstrated that DMPO–$^{\bullet}$OH rapidly decomposes in the presence of the superoxide radical.[44,45] Hence the quantitation of the hydroxyl radical may be of limited value in systems such as phthalocyanines where superoxide is concomitantly produced (Scheme 3).

The Cytochrome c Assay

The reduction of ferricytochrome c at 550 nm[46,47] is a common technique for the detection and quantitation of the superoxide radical anion (1).

$$Fe^{3+}\text{-cytochrome c} + O_2^{\bullet -} \longrightarrow Fe^{2+}\text{-cytochrome c} + O_2 \qquad (1)$$

The calculations of radical yield are based upon different molar absorptivities for the ferricytochrome c ($0.89 \times 10^4\ M^{-1}\,cm^{-1}$) and ferrocytochrome c ($2.9 \times 10^4\ M^{-1}\,cm^{-1}$) with a rate

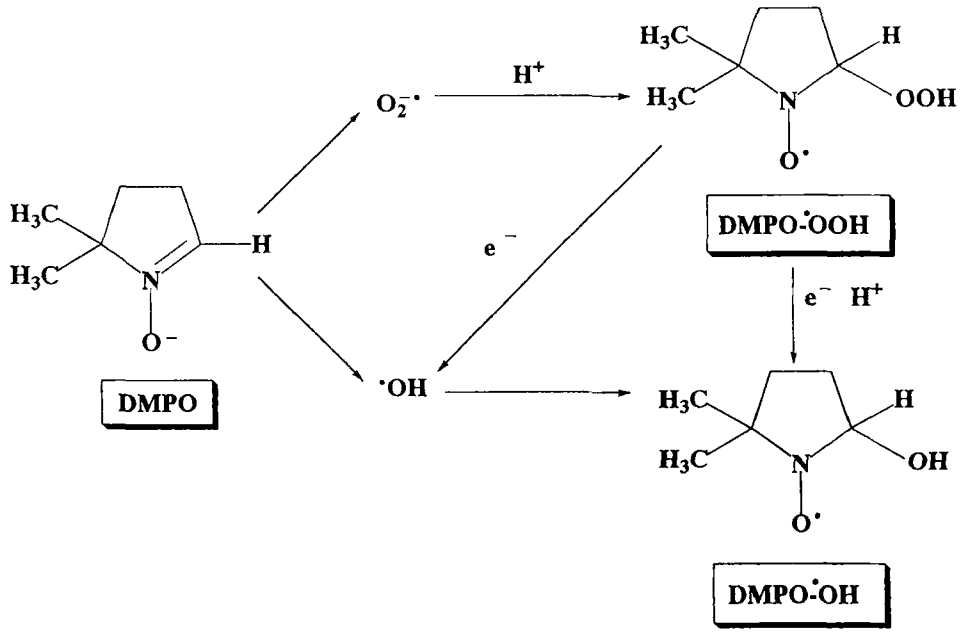

SCHEME 2

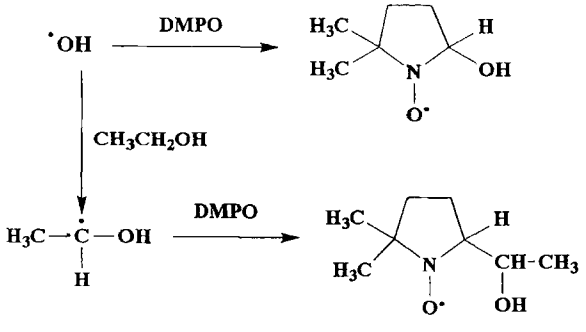

SCHEME 3

constant $k = 1.4 \times 10^6\,M^{-1}\,s^{-1}$ for a pH ranging from 4.7 to 7.4. Despite the possible reduction of ferricytochrome c by other electron donors, the inhibitable effect of SOD selectively discriminates the superoxide radical contribution. A limitation of this method is the possible impact of divalent cations on the superoxide radical dismutation via a Fenton reaction (6),(7) resulting in hydroxyl radicals generation.[48,49] This metallic catalysis may be avoided by treating buffer solutions with a chelating agent such as Chelex. It should be pointed out that, theoretically, dismutation of the superoxide radical may occur in protic solvents via the Haber–Weiss reaction (5). Because the rate constant is very low[48] ($k < 0.3\,M^{-1}\,s^{-1}$) in comparison with the Fenton reaction's rate the contribution of this pathway is usually neglected.

Production of H_2O_2 from $O_2^{\bullet-}$

$$O_2^{\bullet-} \xrightarrow{H^+} HO_2^{\bullet} \xrightarrow{e} HO_2^- \xrightarrow{H^+} H_2O_2 \qquad (2)$$

$$H_2O_2 \xrightarrow{e^-} {}^{\bullet}OH + OH^- \qquad (3)$$

$$HO_2^{\bullet} + HO_2^{\bullet} \longrightarrow H_2O_2 + O_2 \qquad (4)$$

Haber–Weiss reaction

$$O_2^{\bullet-} + H_2O_2 \longrightarrow {}^{\bullet}OH + O_2 + H_2O_2 \qquad (5)$$

Fenton reaction

$$Fe^{3+} + O_2^{\bullet-} \longrightarrow Fe^{2+} + O_2 \qquad (6)$$

$$Fe^{2+} + H_2O_2 \longrightarrow Fe^{3+} + {}^{\bullet}OH + {}^{-}OH \qquad (7)$$

The typical experimental procedure was as follows. DMSO solutions of $ZnPcCl_{16}$ (10^{-5} M) and AlPcCl(10^{-5} M) were freshly prepared before each experiment. Cytochrome c solutions (2.69×10^{-5} M) were made up in chelated phosphate buffer. The final volume for each sample was 3 ml and the water percentage did not exceed 7%. Samples were directly irradiated inside the optical cell. The absorbance of cytochrome c was monitored and recorded at 550 nm every 2 min with a Kontron Uvikon 930 spectrophotometer. Anaerobic experiments were performed after purging samples with argon for 15 min. Quenching experiments were carried out with SOD (40 μg/ml).

RESULTS AND DISCUSSION

Generation of Singlet Oxygen ($^1O_2$) by the Photosensitizers

Formation of TEMPO in Solution

To evaluate the ability of $[(nhex)_3SiO]_2SiPc$, $ZnPcCl_{16}$, $AlPcCl_{16}$, and $HSO_4AlPcCl_{16}$ to generate $^1O_2$, aerated DMF solution of different concentrations of these dyes (2×10^{-5} M, 2×10^{-4} M) were irradiated with white light ($\lambda > 475$ nm) at room temperature after addition of 4-oxo-TEMP (10^{-3} M, 10^{-1} M respectively). However, the two aluminum perchlorinated phthalocyanines are sparingly soluble and must be sonicated before use. Fresh solutions of photosensitizers were prepared before each experiment and we checked that no radical was produced after sonication.[50,51] Thus, we cannot rule out aggregation, favoring dye–dye interactions and thus quenching of $AlPcCl_{16}$ whose foregoing results show that it does not generate $^1O_2$. For comparison, solutions of AlPcCl and 4-oxo-TEMP at the same concentrations as mentioned before were tested.

The spectra evidenced a strong production of 4-oxo-TEMPO nitroxide radical confirming the formation of $^1O_2$ by photoexcited $ZnPcCl_{16}$, HSO_4PcCl_{16} and $[(nhex)_3SiO]_2SiPc$ (Figure 3). When D_2O in which the $^1O_2$ lifetime is lengthened

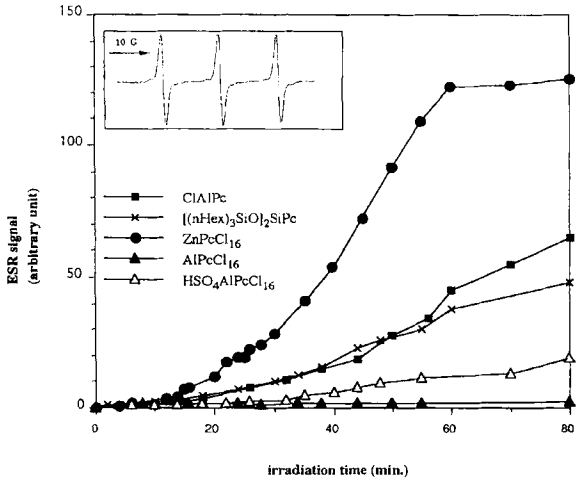

FIGURE 3 Comparative production of 4-oxo-TEMPO radical generated from illumination of DMF phthalocyanines solutions in presence of 4-oxo-TEMP (10^{-3} M). $[(nhex)_3SiO]_2SiPc$ (2×10^{-5} M), $ZnPcCl_{16}$ (2×10^{-5} M), $AlPcCl_{16}$ (2×10^{-5} M), $HSO_4AlPcCl_{16}$ (2×10^{-5} M). Spectrometer settings: microwave: 20 mW; modulation amplitude: 1.243 G; time constant: 40.96 ms, scan rate: 167.772 s; scan width: 100 G, X band, modulation frequency: 100 kHz, receiver gain: 4×10^4.

(decay constant for singlet oxygen k_d (s^{-1}) in water: $2.4–3.2 \times 10^5$, in D_2O: $1.4–2.3 \times 10^4$, in DMF: $4–7.1 \times 10^4$)[52] were added (20%) to the DMF phthalocyanines solutions, ESR signals were 2-fold to 3-fold higher. Along this line, to investigate further the generation of $^1O_2$ upon illumination of our phthalocyanines derivatives, the yield of 4-oxo-TEMPO was studied in the presence of histidine, an animoacid known as singlet oxygen quencher[53] through 1,4 cycloaddition on its imidazole ring (8).

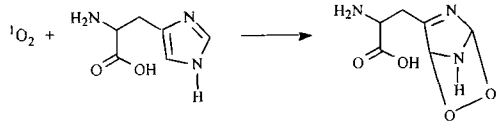

(8)

Figure 4 shows the Stern–Volmer plot of the effect of histidine on the intensities of the 4-oxo-TEMPO radicals upon irradiation of $[(nhex)_3SiO]_2SiPc$, $ZnPcCl_{16}$, $HSO_4AlPcCl_{16}$. Taken together, these results confirm the production of $^1O_2$ by the series of phthalocyanines.

The most efficient new photosensitizers for $^1O_2$ production were $[(nhex)_3SiO]_2SiPc$ and $ZnPcCl_{16}$.

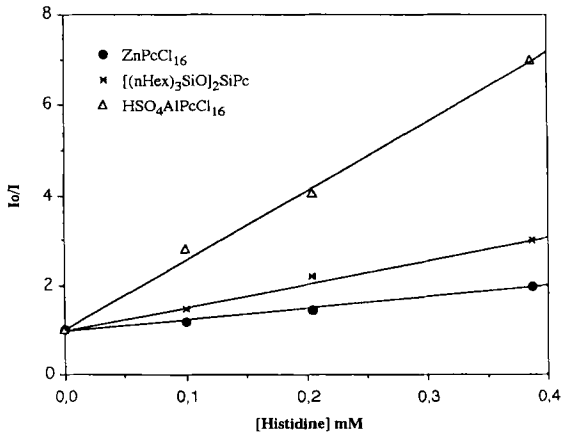

FIGURE 4 Effect of histidine on the intensity of the 4-oxo-TEMPO radical produced upon irradiation of $[(nhex)_3SiO]_2$-SiPc (2×10^{-5} M), $ZnPcCl_{16}$ (2×10^{-5} M), $AlPcCl_{16}$ (2×10^{-5} M). Stern–Volmer plot: I_0/I = ratio of signal intensity in the absence and presence of histidine. Spectrometer settings as in Figure 3.

The zinc phthalocyanine is a powerful source of $^1O_2$, producing higher concentration of 4-oxo-TEMPO than AlPcCl (Figure 3). This result substantiates our hypothesis that chlorination of the sensitizer leads to high $^1O_2$ quantum yields via the heavy atom effect. Heavy atom effects are due to the spin–orbit interaction of an outer-electron (orbital angular momentum l) with the core. ζ_l is the coupling parameter which provides a measure of the strength of the spin–orbit interaction. Heavy atoms show high spin–orbit coupling constants, for instance the ζ_l value for Cl is 587 cm^{-1} whereas H shows a very low coupling constant ($\zeta_l = 0.24\ cm^{-1}$). High spin–orbit interactions usually lead to elevated triplet quantum yields.[54]

TEMPO Formed in Liposomes

Some evidences exist that cell membranes are critical sites affected by photosensitization.[55] Besides, they often play a determinant role in photosensitization photoprocesses, affecting in some cases the photochemical mechanisms.[56,57] Thus, to ensure results obtained in DMF, and to gain more insight into the destructive phototoxic effects, the ESR study of these lipophilic phthalocyanines was extended to the impact of membranes on photochemical processes. Liposomes made from DPPC were used as synthetic membrane models. This saturated phospholipid was selected to avoid the oxidation of unsaturated fatty acid side chains by $^1O_2$ or $^\bullet OH$ and the resulting lipid alkoxyl or peroxyl radicals.

The irradiation of several aerobic dispersions of DPPC liposomes containing $[(nhex)_3SiO]_2SiPc$ at various concentrations (2×10^{-5} M, 2×10^{-4} M) and 4-oxo-TEMP (10^{-3} M, 10^{-1} M respectively) yields strong signals attributable to the formation of 4-oxo-TEMPO. For a given irradiation time, the ESR signals were twice as intense as those observed in DMF (data not shown). On the contrary, after a 30 min irradiation span, very weak signals of 4-oxo-TEMPO were observed for all the perchlorinated phthalocyanines (spectra not shown): signals were found to be 300 times less intense. We checked for all the phthalocyanines, the possible contribution of $O_2^{\bullet -}$ or HO_2^- to the generation of $^1O_2$ using superoxide dismutase (40 μg/ml) and catalase (40 μg/ml). A small effect of these enzymes on the amount of 4-oxo-TEMPO was observed in the borderline of statistical significance (5% decrease of the 4-oxo-TEMPO adduct) (data not shown). Although these enzymes were used at very low doses, histidine, methionine and tryptophan residues of these proteins may be responsible for chemical or $^1O_2$ quenching.[58,59]

The ESR findings seem to be consistent with an increased aggregation of all perchlorinated phthalocyanines in liposomes membranes resulting in the loss of the capacity to generate $^1O_2$. Another possibility is that the lifetime of the singlet or the triplet state of these sensitizers in DPPC membranes considerably decreased.

Generation of Superoxide Radical ($O_2^{\bullet -}$) by the Photosensitizers

DMPO–$^\bullet$OOH Adduct Formed in DMF Solutions

To assess the possible contribution of a Type I mechanism the resulting generation of $O_2^{\bullet -}$ and/or $^\bullet OH$ was investigated. The reaction between

$^3O_2$ and the photosensitizers was studied in presence of the spin-trap: DMPO. This is known to yield a DMPO–•OOH adduct with $O_2^{\bullet-}$ and DMPO–•OH with •OH whose ESR spectra are characteristic.[32,60,61] The superoxide is stable in aprotic solvents such as DMF where disproportionation of $O_2^{\bullet-}$ to •OH via the capture of H^+ is unlikely.[62] When an aerated DMF solution of any of the phthalocyanines studied in this work (2×10^{-5} M, 2×10^{-4} M) was irradiated in presence of DMPO (10^{-1} M), the ESR spectrum observed was assigned to the DMPO–•OOH adduct ($a^N = 12.6$ G, $a_\beta^H = 9.1$ G). The corresponding results for the series of phthalocyanines are given in Figure 5. The non-monotonous behavior of $AlPcCl_{16}$ is probably related to a slow deposit of the compound whose solubility in DMF is obtained only after sonication. Addition of H_2O (20%) in the DMF solutions considerably enhanced the resolution of the spectra. The pattern of the DMPO–•OOH adduct then became more similar to that observed in water displaying the following hyperfine coupling constants: $a^N = 13.1$ G, $a_\beta^H = 12.14$ G and $a_\gamma^H = 1.4$ G (exemplified in Figure 6(b) and (c) with experiments run with

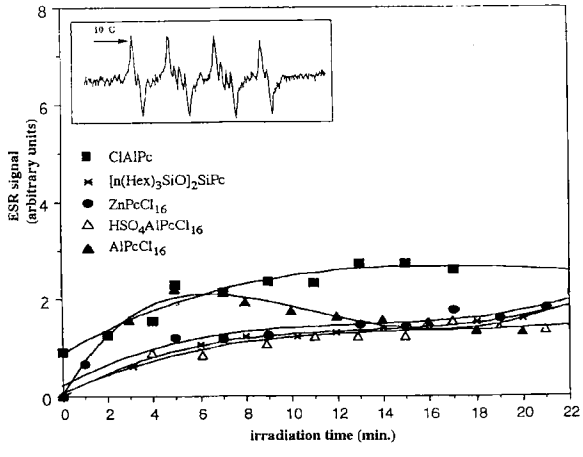

FIGURE 5 Comparative production of DMPO–•OOH radical generated from illumination of DMF phthalocyanines solutions in presence of DMPO (10^{-1} M). $[(nhex)_3SiO]_2SiPc$ (2×10^{-5} M), $ZnPcCl_{16}$ (2×10^{-5} M), $AlPcCl_{16}$ (2×10^{-5} M), $HSO_4AlPcCl_{16}$ (2×10^{-5} M). Spectrometer settings: microwave: 20 mW; modulation amplitude: 1.243 G; time constant: 40.96 ms, scan rate: 167.772 s; scan width: 100 G, X band, modulation frequency: 100 kHz, receiver gain: 8×10^5.

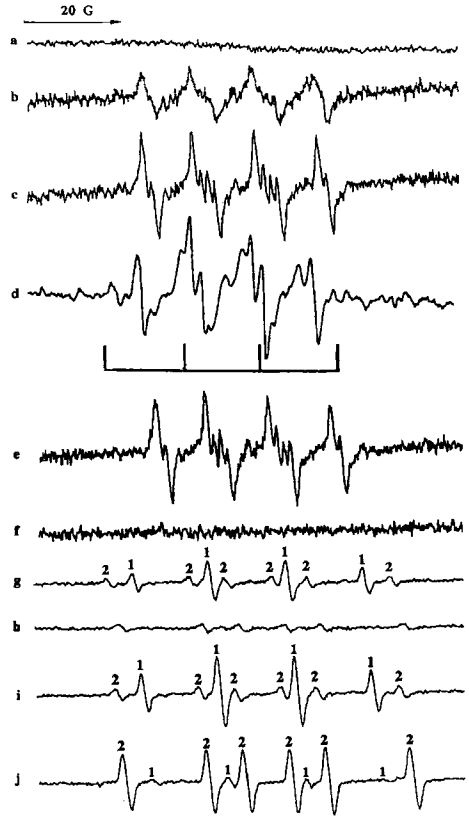

FIGURE 6 ESR spectra of the DMPO–•OOH and DMPO–•OH adducts produced after an irradiation time of 3 min of the system $ZnPcCl_{16}$ (2×10^{-5} M)/DMPO (10^{-1} M). (a) Control run in the dark with $ZnPcCl_{16}$ and DMPO in DMF. (b) DMPO–•OOH adduct produced upon irradiation of $ZnPcCl_{16}$ in presence of DMPO in DMF (receiver gain: 8×10^5). (c) DMPO–•OOH adduct produced upon irradiation of $ZnPcCl_{16}$ in presence of DMPO in a mixture of DMF 80%/water 20% (receiver gain: 8×10^5). (d) DMPO–•OOH (x) and DMPO–•OH (•) adducts produced upon illumination of a liposomal dispersion containing $ZnPcCl_{16}$ and DMPO (receiver gain: 8×10^5). (e) DMPO–•OOH adduct obtained after illumination of a liposomal dispersion containing $ZnPcCl_{16}$, DMPO and desferrioxamine (6×10^{-6} M) (receiver gain 8×10^5). (f) Effect of SOD (40 μg/ml) on the DMPO–•OOH adduct produced upon illumination of a liposomal dispersion containing $ZnPcCl_{16}$ and DMPO (receiver gain 8×10^5). (g) DMPO–•OH adduct formed after an irradiation time of 5 min of the liposomal system previously described (receiver gain 4×10^5). (h) Effect of catalase (40 μg/ml) on the DMPO–•OH adduct formed after an irradiation time of 5 min of the liposomal system previously described (receiver gain 8×10^5). (i) Effect of Fe-DETAPAC (4×10^{-6} M) on the DMPO–•OH adduct produced after an irradiation time of 5 min. of the liposomal system previously described. A DMPO–•R adduct (2) is also detectable (receiver gain 4×10^5). (j) DMPO–•R adduct formed at the expense of the DMPO–•OH adduct (1) after an irradiation time of 20 min of a liposomal dispersion containing $ZnPcCl_{16}$ and DMPO (receiver gain 4×10^5). Spectrometer settings as in Figure 5.

$ZnPcCl_{16}$). Control experiments in dark or in the absence of oxygen showed that the DMPO–•OOH generation is a photodynamic process.

DMPO–•OOH Adduct Formed in Liposomes

In aqueous solution, at pH 7, the rate constant of the reaction[60,61] of DMPO with •OH is approximately $2 \times 10^9\,M^{-1}\,s^{-1}$. Under the same conditions, the rate constant of DMPO with $O_2^{\bullet-}$ is low[60,61]: $10\,M^{-1}\,s^{-1}$. Direct irradiation inside the spectrometer cavity allowed us to observe the DMPO–•OOH adduct formed during the photoexcitation of phthalocyanines. This adduct rapidly decayed in favor of DMPO–•OH (Figure 6(d)). The addition of SOD (40 μg/ml) prior to illumination prevents the formation of DMPO–•OOH, whereas heat denaturated SOD did not modify the ESR spectrum. Moreover, the intensity of the ESR signals were found to be dependent on dye concentration. Catalase and H_2O_2 showed a negligible effect excluding a role of H_2O_2 in the formation of $O_2^{\bullet-}$[40] by photoexcited phthalocyanines (9). We also took into account a possible conversion of $^1O_2$ into $O_2^{\bullet-}$ (10). Neither D_2O, nor histidine had significant effect on the amount of the DMPO–•OOH adduct formed.

$$2H_2O_2 \longrightarrow O_2^{\bullet-} + 2\,{}^{\bullet}OH + 2H^+ \qquad (9)$$

$$^1O_2 + X \longrightarrow O_2^{\bullet-} + X^+ \qquad (10)$$

Irradiation of $AlPcCl_{16}$ and $HSO_4AlPcCl_{16}$ entrapped into liposomes did not generate any detectable DMPO–•OOH adduct (data not shown).

Iron Dependent Production of $O_2^{\bullet-}$ in Liposomes

Previous works have demonstrated that DMPO–•OOH adduct is unstable in the presence of transition metals and easily decomposes into different species, including DMPO–•OH.[32,34,44,60] The efficiency of spontaneous disproportionation of the $O_2^{\bullet-}/HO_2^{\bullet}$ radicals is increased by metallic impurities[61–64] thus causing a strong build up of H_2O_2. Desferrioxamine is a well-known iron chelator preventing further reaction of iron with H_2O_2[23,34,44] preserving thereby the DMPO–•OOH adduct. To avoid any degradation of the DMPO–•OOH produced, desferrioxamine has been added. It was used at low concentration (6×10^{-6} M) to avoid a possible production of free radicals generated by photochemical reaction between phthalocyanine and desferrioxamine.[65] The typical pattern for the DMPO–•OOH adduct with the hyperfine constant values previously reported in water: $a^N = 14.2$ G, $a_\beta^H = 11.2$ G and $a_\gamma^H = 1.25$ G was observed (Figure 6(e)). Control experiments ensured that no signal was obtained without light or O_2. When desferrioxamine was not supplied, the ESR signal amplitude of the DMPO–•OOH adduct weakened rapidly after a few minutes of light exposure, whereas the signal remained constant when chelator was used (Figure 6(d) and (e)).

Formation of Hydroxyl Radical •OH in Liposomes

Transformation of $O_2^{\bullet-}$ into •OH

As previously reported,[14] no DMPO–•OH adduct was observed during irradiation of phthalocyanine solutions neither in DMF nor in mixture of DMF–H_2O (80 : 20). However, photoirradiation at pH 7.4 of an oxygen saturated, liposomal dispersion of phthalocyanines (2×10^{-4} M, 2×10^{-5} M) in the presence of DMPO (10^{-1} M) led to the formation of a large amount of DMPO–•OH spin consisting of the 1 : 2 : 2 : 1 quartet with $a^N = a^H = 14.9$ G[32–66] (Figure 6(g)).

Actually, the DMPO–•OH adduct observed may be deceptive because it may arise from decomposition of DMPO–•OOH[32,34,44,45] thus we checked that catalase (40 μg/ml) or desferrioxamine (6×10^{-6} M) fully inhibited the generation of DMPO–•OH (Figure 6(e) and (h)). This result testifies a primary •OH radical generation from $O_2^{\bullet-}$. A rapid increase in DMPO–•OH yield occurred for an irradiation span of 4 min followed by a plateau in the intensity of the DMPO–•OH

signal 10 min after the beginning of the reaction. These findings are consistent with a predominant $^{\bullet}OH$ formation after mixing of the reagents. The DMPO–$^{\bullet}OH$ signal was still observed 30 min after the end of the irradiation. This result is in agreement with the high stability of the DMPO–$^{\bullet}OH$ adduct whose half-life is about 2 h at pH 7.[32]

Addition of Fe^{3+}–DETAPAC (4×10^{-6} M) increased the formation of the hydroxyl radical (Figure 6(i)). To establish the possible H_2O_2 dependence for the DMPO–$^{\bullet}OH$ generation, control experiments were run in presence of both H_2O_2 and Fe^{3+}–DETAPAC (spectrum not shown). A significant build up occurred, suggesting that the phthalocyanine/O_2 system would be able to generate $^{\bullet}OH$ radicals via the Fenton reaction. H_2O_2 would originate from $O_2^{\bullet-}$ as in reaction (2) or (4) or from dismutation of $O_2^{\bullet-}$ both followed, in the presence of Fe^{2+} by reaction (7).

When ESR signals were recorded, a second distinct figure corresponding to a DMPO–$^{\bullet}R$ radical was observed (Figure 6(i) and (j)). The trapped species may be an abstraction radical from DMF or DPPC formed by $^{\bullet}OH$ attack (11),(12). Another possibility is the degradation of DMPO.[33–66] The observed hyperfine coupling constants of this adduct are the following: $a^N = 16.33$ G, $a_\beta^H = 23$ G.

$$(CH_3)_2NCHO + {}^{\bullet}OH \longrightarrow {}^{\bullet}CH_2N(CH_3)CHO + H_2O \quad (11)$$

$$^{\bullet}CH_2N(CH_3)CHO + DMPO \longrightarrow DMPO\text{–}{}^{\bullet}CH_2N(CH_3)CHO \quad (12)$$

Finally, experiments run in liposomal dispersions did not provide clear evidence of an influence of electron donating molecules on the DMPO–$^{\bullet}OOH$ or the DMPO–$^{\bullet}OH$ generation (data not shown).

Proposed Mechanisms for the Production of $O_2^{\bullet-}$

Phthalocyanine excitation by red light and intersystem crossing, allow simultaneously both oxygen dependent Type I and Type II mechanisms. The following electron transfer reactions can be involved:

$$Pc + h\nu \longrightarrow {}^1Pc^* \longrightarrow {}^3Pc^* \quad (13)$$

$$^3Pc^* + {}^3O_2 \longrightarrow Pc + {}^1O_2 \quad (14)$$

$$^3Pc^* + Pc \longrightarrow Pc^{\bullet-} + Pc^{\bullet+} \quad (15)$$

$$^3Pc^* + D \longrightarrow Pc^{\bullet-} + D^{\bullet+} \quad (16)$$

$$Pc^{\bullet-} + O_2 \longrightarrow Pc + O_2^{\bullet-} \quad (17)$$

$$^3Pc^* + O_2 \longrightarrow Pc^{\bullet+} + O_2^{\bullet-} \quad (18)$$

In process (14) the triplet formed during irradiation collides with molecular oxygen to generate $^1O_2$ whereas in process (15) the phthalocyanine in the triplet state collides with another phthalocyanine molecule in the ground state, leading to an electron transfer. The resulting $Pc^{\bullet-}$ anion radical then gives in turn its electron to dioxygen, producing $O_2^{\bullet-}$ (17). $Pc^{\bullet-}$ can be also produced by process (16): an electron donor D can transfer an electron to the excited state $^3Pc^*$ and gets to $Pc^{\bullet-}$. Alternatively the possibility that $^3Pc^*$ may transfer an electron to dioxygen and generate $O_2^{\bullet-}$ (process (18)) cannot be discarded.

The possible involvement of a phthalocyanine radical derivative was confirmed for $ZnPcCl_{16}$. When the crystallized form of the photosensitizer was irradiated, a one broad line ESR signal was observed (Figure 7). Control experiments showed that light was necessary to produce this signal. We were unable to observe the corresponding DMPO adduct in anaerobic DMF solutions nor in deaerated liposomal suspensions. This signal was assumed to result from phthalocyanine derivative radical occurring during photosensitization as in reactions (13), (15).

Other phthalocyanines, neither crystallised nor in solution, were not able to generate any detectable radical when irradiated.

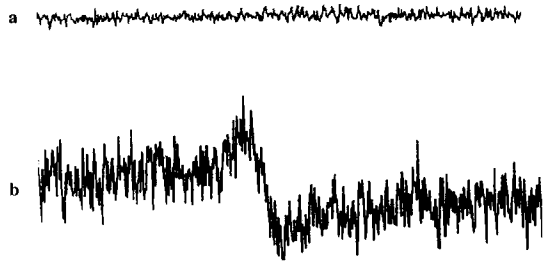

FIGURE 7 ESR spectrum of $ZnPcCl_{16}$ radical obtained upon irradiation of the crystallized dye. Spectrometer settings: microwave: 20 mW; modulation amplitude: 1.243 G; time constant: 40.96 ms, scan rate: 167.772 s; scan width: 100 G, X band; modulation frequency: 100 kHz; receiver gain: 8×10^5 (a) Control run in the dark, (b) signal obtained upon illumination.

Quantitation of the Superoxide Radical

ESR Technique

Though the spin-trapping of the superoxide radical using DMPO is very sensitive, it may be deceptive for truly accurate quantitation in view of a possible rapid decay of spin-adducts. Actually spin-adducts in DMF were stable exhibiting long life-time (over 30 min). This feature allowed us to compare results from ESR experiments along with the data obtained at levels where a linear measurement is obtained with the cytochrome c reduction assay. Results are shown in Table II.

Cytochrome c Assay

The use of cytochrome c to quantify the production of $O_2^{\bullet -}$ was carried out with only two phthalocyanines, namely AlPcCl and $ZnPcCl_{16}$. The other phthalocyanines were either unstable in DMSO ($[(nhex)_3SiO]_2SiPc$) or soluble only in DMF ($AlPcCl_{16}$, and $HSO_4AlPcCl_{16}$) in which the cytochrome c is unstable. Precise amounts of $O_2^{\bullet -}$ production were obtained from the comparison between anaerobic and aerobic experiments, permitting to estimate the level of ferrocytochrome c due to a direct electron transfer from phthalocyanines in the excited state. The amounts of $O_2^{\bullet -}$ trapped by ferrocytochrome c are given in Table II. Quenching experiments of $O_2^{\bullet -}$ were performed with native and heat denaturated SOD. The enzymatic assay (data not shown) as well as anaerobic experiments showed that reduction of cytochrome c was essentially due to $O_2^{\bullet -}$ (Figure 8). Control experiments ensured that no reduction occurred in absence of irradiation.

TABLE II ESR and cytochrome c assays: comparative quantitation of $O_2^{\bullet -}$ produced by irradiation of the studied phthalocyanines

Photosensitizer	$nO_2^{\bullet -}$ (10^{-6} M) (irradiation time: 5 min)	$nO_2^{\bullet -}$ (10^{-6} M) (irradiation time: 5 min)
	ESR quantitation	Cytochrome c assay
ClAlPc	2.2	1.8
$[(nhex)_3SiO]_2SiPc$	1	—
$ZnPcCl_{16}$	1	0.7
$AlPcCl_{16}$	0.8	—
$HSO_4AlPcCl_{16}$	0.7	—

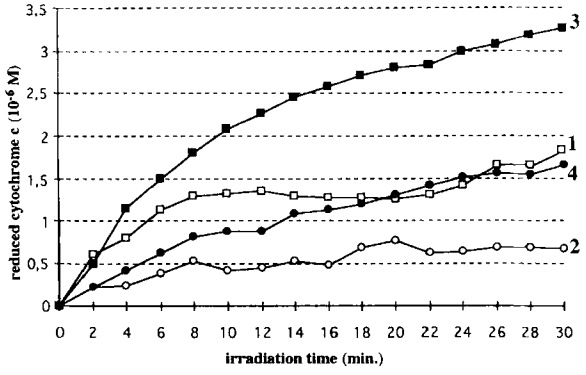

FIGURE 8 Comparative yield of reduced cytochrome c obtained from systems containing cytochrome c (2.69×10^{-5} M) and $ZnPcCl_{16}$ (2×10^{-5} M) (1 and 2) or AlClPc (2×10^{-5} M) (3 and 4). Yields are given for aerobic conditions (1 and 3) and anaerobic conditions (2 and 4).

CONCLUSION

Our ESR experiments show that phthalocyanines which exhibit potentialities as photosensitizer for PDT of melanotic and leukemic cells, are able to operate by Type I and Type II pathways in DMF. The two mechanisms occur simultaneously although the Type II seems to be prevalent. These results are not changed when the bis(tri-*n*-hexylsiloxy) silicon phthalocyanine is entrapped into

liposomes. By contrast, for all the perchlorinated phthalocyanines the Type I process is still favored in membrane models whereas the Type II pathway is negligible. It is likely that this modified photophysical behavior is due to a possible stacking of phthalocyanines in membranes. These findings suggest that in the case of the bis(tri-*n*-hexylsiloxy) silicon phthalocyanine the photochemical processes remain unmodified in DMF and in liposomal dispersions because of the preventing effect of axial ligands against aggregation. A significant increase of the Type II contribution was observed in liposomes. Perchlorinated phthalocyanines are devoid of a Type II mechanism contribution when these photosensitizers are incorporated into liposomes where the photoinduced electron-transfer pathway is still favored. Results obtained with the zinc perchlorinated phthalocyanine indicate that photodynamic action of this compound is not dependent on $^1O_2$. Phototoxicity of this compound would be essentially mediated by oxygen free radicals. The experiments related to the presence or absence of $^{\bullet}OH$ radicals demonstrate that during irradiation of air saturated liposomal suspension of phthalocyanines, the generation of $^{\bullet}OH$ is iron dependent and originates from $O_2^{\bullet -}$ or its protonated form $^{\bullet}O_2H$[62,67–69] via the Fenton reaction.

Quantitative results obtained from the cytochrome c reduction and the ESR techniques are in good agreement. Problems usually encountered when trying to quantify $O_2^{\bullet -}$, namely disproportionation of the superoxide radical or degradation of the spin-trap seem avoided in aprotic solvents such as DMF and DMSO.

Acknowledgements

One of us (A. Viola) thanks La Ligue Nationale Contre le Cancer for financial help.

References

[1] M. Jin, B. Yang, W. Zhang and Y. Wang (1994). Photodynamic therapy for upper gastrointestinal tumours over the past 10 years. *Seminars in Surgical Oncology*, **10**: 111–113.

[2] T.C. Origitano, M.J. Caron and O.H. Reichman (1994). Photodynamic therapy for intracranial neoplasms. Literature review and institutional experience. *Molecular and Chemical Neuropathology*, **21**: 337–352.

[3] H.I. Pass and J.S. Donington (1995). Use of photodynamic therapy for the management of pleural malignancies. *Seminars in Surgical Oncology*, **11**: 360–367.

[4] M.A. Biel (1995). Photodynamic therapy of head and neck cancers. *Seminars in Surgical Oncology*, **11**: 355–359.

[5] J.S. Nelson, L.H. Liaw and M.W. Berns (1987). Tumor destruction in photodynamic therapy. *Photochemistry and Photobiology*, **46**: 829–835.

[6] T.J. Dougherty (1993). Photodynamic therapy. *Photochemistry and Photobiology*, **58**: 895–900.

[7] J. Moan and K. Berg (1992). Photochemotherapy of cancer: Experimental research. *Photochemistry and Photobiology*, **55**: 931–948.

[8] C.J. Gomer (1991). Preclinical examination of first and second generation photosensitizers used in photodynamic therapy. *Photochemistry and Photobiology*, **54**: 1093–1107.

[9] B.W. Henderson and T.J. Dougherty (1992). How does photodynamic therapy work? *Photochemistry and Photobiology*, **55**: 145–157.

[10] G. Laustriat (1986). Molecular mechanisms of photosensitization. *Biochimie*, **68**: 771–778.

[11] M.A. Fox (1990). Photoinduced electron transfer. *Photochemistry and Photobiology*, **52**: 617–627.

[12] C.S. Foote (1990). Chemical mechanisms of photodynamic action, *Proceedings of SPIE Institute "Advanced Optical Technologies on Photodynamic Therapy"*, **IS6**: 115–126.

[13] L.I. Grossweiner, A.S. Pavel and J.B. Grossweiner (1982). Type I and Type II mechanisms in the photosensitized lysis of phosphatidylcholine liposomes by hematoporphyrin. *Photochemistry and Photobiology*, **36**: 159–167.

[14] E. Ben-Hur, A. Carmichael, P. Riesz and I. Rosenthal (1985). Photochemical generation of superoxide radical and the cytotoxicity of phthalocyanines. *International Journal of Radiation Biology*, **48**: 837–846.

[15] I. Rosenthal, C. Murali Krishna, P. Riesz and E. Ben-Hur (1986). The role of molecular oxygen in the photodynamic effect of phthalocyanines. *Radiation Research*, **107**: 136–142.

[16] Z. Zhiyi, W. Nenghui, W. Quian and L. Meifan (1993). EPR studies of singlet oxygen ($^1O_2$) and free radicals ($O_2^{\bullet -}$, $OH^{\bullet}$, $HB^{\bullet -}$) generated during photosensitization of Hypocrellin B. *Free Radical in Biology and Medicine*, **14**: 1–9.

[17] Z. Diwu and W. Lown (1994). Photosensitization with anticancer agents 19. EPR studies of photodynamic action of Calphostin C: Formation of semiquinone radical and activated oxygen on illumination with visible light. *Free Radical in Biology and Medicine*, **16**: 645–652.

[18] C. Hadjur, A. Jeunet and P. Jardon (1994). Photosensitization by hypericin: ESR evidence for singlet oxygen and superoxide anion radicals formation in an *in vitro* model. *Journal of Photochemistry and Photobiology B: Biology*, **26**: 67–74.

[19] M.S. Patterson, S.J. Madsen and B.C. Wilson (1990). Experimental tests on the feasibility of singlet oxygen luminescence monitoring *in vivo* during photodynamic therapy. *Journal of Photochemistry and Photobiology B: Biology*, **5**: 69–84.

[20] A.A. Gorman and M.A.J. Rodgers (1992). Current perspectives of singlet oxygen detection in biological

environments. *Journal of Photochemistry and Photobiology B: Biology*, **14**: 159–176.
[21] A. Baker and J.R. Kanofsky (1993). Time resolved of singlet oxygen emission from L1210 leukemia cells labeled with 5-(N-hexadecanoyl)amino eosin. A comparison with one dimensional model of singlet oxygen diffusion and quenching. *Photochemistry and Photobiology*, **57**: 720–727.
[22] T.G. Gantchev (1992). Spin-trapping of free radicals during phthalocyanine photosensitization of lymphoma cells *in vitro*. *Cancer Biochemistry and Biophysics*, **13**: 103–111.
[23] S.I. Liochev and I. Fridovich (1994). The role of $O_2^{\bullet -}$ in the production of $HO^{\bullet}$ *in vitro* and *in vivo*. *Free Radical in Biology and Medicine*, **16**: 29–33.
[24] I. Rosenthal and E. Ben-Hur (1992). Ascorbate assisted phthalocyanine-sensitized photohaemolysis of human erythrocytes. *International Journal of Radiation Biology*, **62**: 481–486.
[25] H. Kim, I. Rosenthal, L.J. Kirschenbaum and P. Riesz (1992). Photosensitized formation of ascorbate of radicals by chloroaluminum phthalocyanine tetrasulfonate: an electron spin resonance study. *Free Radical in Biology and Medicine*, **13**: 231–238.
[26] T.G. Gantchev, I.J. Urumov, J.E. Hunting and J.E. Van Lier (1995). Phototoxicity and intracellular generation of free radicals by tetrasulphonated Al– and Zn–phthalocyanines. *International Journal of Radiation Biology*, **65**: 289–298.
[27] J.P. Daziano, S. Steenken, C. Chabannon, P. Mannoni, M. Chanon and M. Julliard (1996). Photophysical and redox properties of a series of phthalocyanines. Relation with their photodynamic activities on TF-1 and DAUDI leukemic cells. *Photochemistry and Photobiology*, **64**: 712–719.
[28] R. Decréau, A. Viola, C. Hadjur, M.-J. Richard, A. Jeunet, A. Favier and M. Julliard (1997). Photothérapie dynamique: étude des potentialités anti-tumorales de la bis (tri *n*-hexyl siloxy) phtalocyanine de silicium sur mélanocytes malins achromiques M6. *Comptes Rendus de la Société de Biologie*, **191**: 639–657.
[29] B.L. Wheeler, G. Nagasubramanian, A.L. Bard, L.A. Schechtman, D.R. Dininny and M.E. Kenney (1984). A silicon phthalocyanine and a silicon naphthalocyanine synthesis, electrochemistry, and electrogenerated chemiluminescence. *Journal of the American Chemical Society*, **106**: 7404–7410.
[30] N. Brasseur, T.-L. Nguyen, R. Langlois, R. Ouellet, S. Marengo, D. Houde and J.E. Van Lier (1994). Synthesis and photodynamic activities of silicon 2,3-naphthalocyanine derivatives. *Journal of Medicinal Chemistry*, **37**: 415–420.
[31] M.N. Golovin, P. Seymour, K. Jayaraj, Y.S. Fu and A.B. Lever (1990). Perchlorinated phthalocyanines: spectroscopic properties and surface electrochemistry. *Inorganic Chemistry*, **29**: 1719–1727.
[32] G.R. Buettner and L.W. Oberley (1978). Considerations in the spin-trapping of superoxide and hydroxyl radical in aqueous system using 5,5 dimethyl-1-pyrroline oxide. *Biochemical and Biophysical Research Communications*, **83**: 69–74.
[33] K. Makino, H. Imaishi, S. Morinishi, T. Hagiwara and T. Takeuchi (1988). An artifact in the ESR spectrum obtained by spin-trapping with DMPO. *Free Radical Research Communications*, **6**: 19–28.
[34] M.J. Burkitt (1993). ESR spin trapping studies of the nature of oxidizing species formed in the Fenton reaction: pitfalls associated with the use of 5,5-dimethyl-1-pyrroline-N-oxide in the detection of the hydroxyl radical. *Free Radical Research Communications*, **18**: 43–57.
[35] G. Strul, A.A. Frimer and L. Weiner (1993). Spin-trapping of free radical penetration into liposomal membranes. *Journal of Chemical Society Perkin Transactions*, **2**: 2057–2059.
[36] S. Batzri and E.D. Korn (1980). Single bilayer liposomes prepared without sonication. *Biochimica et Biophysica Acta*, **594**: 53–84.
[37] A. Viola, C. Hadjur, A. Jeunet and M. Julliard (1996). EPR evidences of superoxide ($O_2^{\bullet -}$) and hydroxyl ($^{\bullet}OH$) radicals by irradiation of a new PDT photosensitizer: Victoria Blue BO. *Journal of Photochemistry and Photobiology. B: Biology*, **32**: 49–58.
[38] Y. Lion, M. Delmelle and A. Van de Vorst (1976). New method of detecting singlet oxygen production. *Nature*, **263**: 442–443.
[39] J. Moan and E. Wold (1979). Detection of singlet oxygen by ESR. *Nature*, **279**: 450–451.
[40] S. Dzwigaj and H. Pezerat (1995). Singlet oxygen-trapping as a method of $^1O_2$ detection: role of some reducing agent. *Free Radical Research Communications*, **23**: 103–115.
[41] J.R. Harbour and M.L. Hair (1978). Detection of superoxide ions in nonaqueous media. Generation by photolysis of pigment dispersions. *Journal of Physical Chemistry*, **82**: 1397–1399.
[42] P.L. Hall (1972). Errors in the determination of ESR spin concentrations by numerical double integration. *Journal of Physics D: Applied Physics*, **5**: 673–675.
[43] E. Finkelstein, G.M. Rosen and E.J. Rauckman (1981). Production of hydroxyl radical by decomposition of superoxide spin-trapped adducts. *Molecular Pharmacology*, **21**: 262–265.
[44] G.R. Buettner (1993). The spin-trapping of superoxide and hydroxyl free radicals with DMPO (5,5 dimethyl pyrroline-N-oxide): more about iron. *Free Radical Research Communications*, **19**: S79–S87.
[45] S. Pou, M.S. Cohen, B.E. Britigan and G.M. Rosen (1989). Spin-trapping and human neutrophils. Limits of detection of hydroxyl radical. *Journal of Biological Chemistry*, **264**: 12299–12302.
[46] J.G. Buttler, G. Jayson and A.J. Swallow (1975). The reaction between the superoxide anion radical and cytochrome c. *Biochimica et Biophysica Acta*, **408**: 215–222.
[47] H. Seki, Y.A. Ilan, Y. Ilan and G. Stein (1976). Reaction of the ferri–ferrocytochrome-c system with superoxide/oxygen system and CO_2^-/CO_2 studied by fast pulse radiolysis. *Biochimica et Biophysica Acta*, **440**: 573–586.
[48] W.H. Koppenol, K.J.H. Van Buuren, J. Buttler and R. Braams (1976). The kinetics of the reduction of cytochrome c by the superoxide anion radical. *Biochimica et Biophysica Acta*, **449**: 157–168.
[49] S.P. Sanders, S.J. Harrisson, P. Kuppusamy, J.T. Sylvester and J.L. Zweier (1994). A comparative study of EPR spin-trapping and cytochrome c reduction techniques for the measurement of superoxide anions. *Free Radical in Biology and Medicine*, **16**: 753–761.
[50] K. Makino, M. Mossoba and P. Riesz (1982). Chemical effect of ultrasound on aqueous solutions. Evidence for $^{\bullet}OH$ and $^{\bullet}H$ spin-trapping. *Journal of the American Chemical Society*, **104**: 3537–3539.
[51] V. Misik and P. Riesz (1996). Peroxyl radical formation in aqueous solutions of N,N dimethylformamide and

dimethylsulphoxide by ultrasound: implications for sonosensitized cell killing. *Free Radical in Biology and Medicine*, **20**: 129–138.

[52] F. Wilkinson, W.P. Helman and A.B. Ross (1993). Rate constants for the decay and reactions of the lowest electronically excited singlet state of molecular oxygen in solution. An expanded and revised compilation. *Journal of Physical and Chemical Reference Data*, **24**: 663–1019.

[53] T.A. Dahl (1992). Pharmacological implications of photosensitization and singlet oxygen toxicity. *International Journal of Immunopharmacology*, **5**: 57–62.

[54] S.L. Murov, I. Carmichael and G.L. Hug (1993). In *Handbook of Photochemistry*, second edition, M. Dekker inc., New-York, Basel, Hong-Kong, pp. 338–341.

[55] D.P. Valenzano (1987). Photomodification of biological membranes with emphasis on singlet oxygen mechanisms. *Photochemistry and Photobiology*, **46**: 147–160.

[56] A.W. Girotti (1990). Photobiology school. Photodynamic lipid peroxidation in biological systems. *Photochemistry and Photobiology*, **51**: 497–509.

[57] P.E. Hartman, W. Dixon, T.A. Dahl and M.E. Daub (1988). Multiple modes of photodynamic action by Cercosporin. *Photochemistry and Photobiology*, **47**: 699–703.

[58] N. Suzuki, I. Mizumuto, Y. Toya, T. Nomoto, S. Mashiko and H. Inaba (1990). Steady-state near infrared detection of singlet molecular oxygen: a Stern–Volmer plot quenching experiment with luminol, superoxide dismutase, and *Cypridina* luciferin analogues. *Agricultural and Biological Chemistry*, **54**: 2783–2787.

[59] B. Halliwell and J.M.C. Gutteridge (1989). In *Free Radicals in Biology and Medicine*, second edition, Oxford University Press, New York, p. 148.

[60] E. Finkelstein, G.M. Rosen and E.J. Rauckman (1980). Spin-trapping of superoxide and hydroxyl radical: practical aspects. *Archives of Biochemistry and Biophysics*, **200**: 1–16.

[61] E. Finkelstein, G.M. Rosen and E.J. Rauckman (1980). Spin-trapping. Kinetics of the reaction of superoxide and hydroxyl radicals with nitrones. *Journal of the American Chemical Society*, **102**: 4994–4999.

[62] C. Ferradini (1986). Espèces activées radicalaires de l'oxygène. *Biochimie*, **68**: 779–785.

[63] H.J. Bielski, D.E. Cabelli and R.L. Arudi (1985). Reactivity of $O_2^{\bullet -}/HO_2^{\bullet}$ radicals in aqueous solution. *Journal of Physical and Chemical Reference Data*, **14**: 1041–1051.

[64] E. Finkelstein, G.M. Rosen and E.J. Rauckman (1989). Problems associated with spin-trapping of oxygen centered free radicals in biological systems. *Analytical Biochemistry*, **177**: 1–6.

[65] A.S.W. Li, A.H. de Haas, C.F. Chignell and A.G. Motten (1989). Superoxide dismutase amplifies dye photosensitized production of desferal free radical: an electron spin-resonance study. *Biochemical and Biophysical Research Communications*, **160**: 1055–1060.

[66] G. Buettner (1987). Spin-trapping: ESR parameters of spin adducts. *Free Radical in Biology Medicine*, **3**: 259–303.

[67] M.J. Davies, L.G. Forni and S.L. Shuter (1987). Electron spin resonance and pulse radiolysis studies on the spin-trapping of sulphur-centered radicals. *Chemical Biological Interactions*, **61**: 177–188.

[68] B. Halliwell and J.M.C. Gutteridge (1986). Oxygen free radicals and iron in relation to biology and medicine some problems and concepts. *Archives of Biochemistry and Biophysics*, **246**: 501–514.

[69] D.T. Sawyer and J.S. Valentine (1981). How super is superoxide? *Accounts of Chemical Research*, **14**: 393–400.